

# Balanced Constrained Carbon Equilibrium Accompanied by Carbide Precipitation



F.M. CASTRO CERDA, C. GOULAS, and L.A.I. KESTENS

The final carbon content of austenite in equilibrium with tempered martensite can be estimated by the so-called constrained carbon equilibrium in the presence of carbide (CCE $\theta$ ) model. However, the linear predictions under CCE $\theta$  deviate from both the initial and the experimentally measured carbon content. A modified approach to the CCE $\theta$  model is proposed, which predicts an increase of the carbon content in austenite with the decrease of temperature below the onset of martensitic transformation.

<https://doi.org/10.1007/s11661-021-06240-6>

© The Minerals, Metals & Materials Society and ASM International 2021

THE aim of quenching and partitioning (Q&P) of carbon steel is to produce a microstructure consisting primarily of martensite and stabilized austenite. The stabilization of austenite is achieved via carbon migration from martensite during the partitioning stage. This framework was probably the inspiration of Speer *et al.*<sup>[1]</sup> to propose an expression whereby the final carbon content of austenite (and the maximum fraction of stable austenite) is estimated under a constrained carbon equilibrium (termed CCE) condition between martensite and austenite. The CCE model is, thus, expressed under the conditions

$$\mu_C^{\alpha'} = \mu_C^{\gamma} \quad [1]$$

$$\mu_{Fe}^{\alpha'} \neq \mu_{Fe}^{\gamma} \quad [2]$$

$$X_C^{\alpha'} \times f_V^{\alpha'} + X_C^{\gamma} \times f_V^{\gamma} = X_C^0 \quad [3]$$

where  $\mu_i^k$  is the chemical potential of  $i$  in the phase  $k$ ,  $X_i^k$  is the mole fraction of  $i$  in the phase  $k$ , and  $f_V^k$  is the volume fraction of the phase  $k$ .  $X_C^0$  represents the

initial composition of the system in mole fraction. Metallographic observation of typical microstructures of low carbon steel subjected to Q&P will readily indicate that a suitable thermodynamic description of the system should consider the equilibrium between martensite, austenite, and carbide (see, for example<sup>[2-4]</sup>). Toji *et al.*<sup>[3]</sup> proposed a modification of the original CCE model by Speer *et al.*<sup>[1]</sup> considering the equilibrium of austenite with tempered martensite, the so-called CCE $\theta$  model. The degree of carbon enrichment of austenite is, thus, calculated in the latter after the precipitation of carbides in martensite (suggested to occur under paraequilibrium, PE, conditions). The CCE $\theta$  model is defined under the main constraint

$$\mu_C^{\alpha'} = \mu_C^{\theta} = \mu_C^{\gamma} \quad [4]$$

Notice that the model by Toji *et al.* does not take into account the mass balance of carbon. Adding the condition that carbon must be balanced between the three phases, i.e.,

$$X_C^{\alpha'} \times f_V^{\alpha'} + X_C^{\theta} \times f_V^{\theta} + X_C^{\gamma} \times f_V^{\gamma} = X_C^0 \quad [5]$$

one can estimate the equilibrium in a mixture of tempered martensite and austenite based on key features of both previous models, namely, (i) the equilibrium of  $\alpha'$ ,  $\theta$ , and  $\gamma$  and (ii) the mass balance. This new approach shall be called BCE $\theta$  thereon. In computing the carbon content of austenite ( $X_C^{\gamma}$ ) under CCE, it is promptly realized that the carbon content increases as the temperature decreases below the  $M_S$ . Combining Eqs. [4] and [5] in<sup>[1]</sup> and solving for  $X_C^{\gamma}$  gives

$$X_C^{\gamma} = (X_C^0 - X_C^{\alpha'} \times f_V^{\alpha'}) \times (1 - f_V^{\alpha'})^{-1} \quad [6]$$

$X_C^{\alpha'}$  estimated under PE between BCC and FCC phases is usually very small, and  $f_V^{\alpha'}$  grows

F.M. CASTRO CERDA is with the Department of Metallurgy, University of Santiago de Chile, Alameda 3363, 9170022 Estacion Central, Santiago, Chile and also with Department of Materials Science and Engineering, Delft University of Technology, Mekelweg 2, 2628CD, Delft, The Netherlands. Contact e-mail: felipe.castro@usach.cl. C. GOULAS is with the Department of Materials Science and Engineering, Delft University of Technology and also with Department of Design production and management, Faculty of Engineering Technology (ET), University of Twente, Drienerlolaan 5, 7522NB Enschede, The Netherlands. L.A.I. KESTENS is with the Department of Materials Science and Engineering, Delft University of Technology and also with Department of Electromechanical Systems and Materials, Research Group Materials Science and Technology, Ghent University, Tech Lane Science Park Campus A 46, Gent, Belgium.

Manuscript submitted October 27, 2020; accepted March 8, 2021.

Article published online April 5, 2021

exponentially<sup>[5]</sup> as T decreases. Hence the expression is reduced to a constant divided by a factor which approaches to zero as the temperature decreases. A similar expression for  $X_C^\gamma$  is obtained from BCE $\theta$  model (Eq. [5]), whence

$$X_C^\gamma = (X_C^0 - X_C^\alpha \times f_V^\alpha - X_C^\theta \times f_V^\theta) \times (1 - f_V^\alpha - f_V^\theta)^{-1} \quad [7]$$

For  $X_C^\alpha \approx 0$ ,  $X_C^\gamma$  is virtually constant and  $f_V^\theta$  grows relatively slowly with decreasing temperature. Eq. [7] predicts a rather slower increment in  $X_C^\gamma$ , compared with CCE as the temperature decreases, by virtue of the factor  $X_C^\theta \cdot f_V^\theta$ . Comparison of Eqs. [6] and [7] indicates that (i)  $X_C^\gamma$  increases as the temperature decreases in both models and (ii)  $X_{C,CCE}^\gamma > X_{C,BCE\theta}^\gamma$  for  $T < M_S$ .

The solid black lines in Figure 1 show the calculation of CCE and BCE $\theta$  for a system of composition similar to that reported by Toji *et al.*<sup>[3]</sup> (1.07C-2.9Mn-2.2Si in wt. percent of C). The inferences (i) and (ii) made on the previous paragraph are consistent with the calculations shown in Figure 1. Calculations were run using ThermoCalc software, version 2020a, database TCFE9.  $X_C^\gamma$  under BCE $\theta$  was estimated for a  $\alpha'/\theta$  paraequilibrium when only C was the diffusing element (outlined circles in Figure 1), and when both C and Si (cross-circles in Figure 1) were allowed to partition. Despite that Toji *et al.*<sup>[3]</sup> do not elaborate on why their prediction yields  $X_{C,CCE}^\gamma < X_{C,CCE\theta}^\gamma$  for temperatures slightly below  $M_S$ , (or for low fractions of martensite, as in their plot); it should be noticed that their model predicts a

hypothetical transition from  $\alpha' + \gamma$  equilibrium at low martensitic contents (slightly below the  $M_S$ ) to  $\alpha' + \gamma + \theta$  equilibrium. Notice also that both CCE $\theta$  calculi in<sup>[3]</sup> in fact predict a largely overestimated  $X_C^\gamma$  value at low temperatures (dashed blue curves in Figure 1). They argued that the CCE $\theta$  prediction should give a constant  $X_C^\gamma$  with temperature, based on the construction of the Gibbs free energy curves for the equilibrium between martensite, cementite, and austenite. The constant  $X_C^\gamma$  reported by Toji *et al.*<sup>[3]</sup> arises from the argument that the chemical potential of carbon in both martensite and austenite is equal during partitioning; thus, a change in the fraction of martensite with temperature should not influence  $X_C^\gamma$ . This is actually true whenever the system is allowed to adjust the phase fractions according to the mass balance, i.e.,  $f_V^\alpha$ ,  $f_V^\gamma$ , and  $f_V^\theta$ . In the case of Q&P, it is considered that the phase fractions are fixed; thus, the degrees of freedom left to the system to attain equilibrium are  $X_C^\alpha$  and  $X_C^\gamma$  ( $X_C^\theta$  is constant). Consequently, the final carbon content in austenite (the predicted  $X_{C,CCE\theta}^\gamma$ ) should not be solely estimated from the condition  $\mu_C^\alpha = \mu_C^\gamma$ . To illustrate this, Figure 2 (black solid line) shows the temperature variation of  $\mu_C$  for a system similar to that studied by Toji *et al.*<sup>[3]</sup> The carbon content of austenite under PE with tempered martensite, as estimated from  $\mu_C$ , is shown as a dashed blue line in Figure 2. Finally, the initial carbon content calculated from the mass balance ( $X_{C-\mu_C}^0$  in Eq. [2]) correspond to the solid blue line in Figure 2. The overestimation of C content which arises from determining  $X_C^\gamma$  under CCE $\theta$  from the condition  $\mu_C^\alpha = \mu_C^\gamma$  becomes evident when comparing the actual initial composition (red dashed line in Figure 2), with the recalculated average carbon content values under the same condition. Else,  $\mu_C^\alpha = \mu_C^\gamma$  yields values of  $X_C^\gamma$  unrealistically high (cf. solid blue line

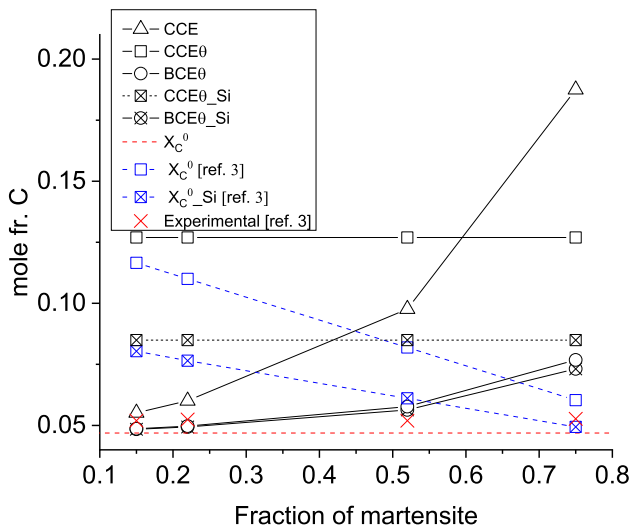


Fig. 1—CCE, CCE $\theta$ , and BCE $\theta$  calculations of carbon content in austenite ( $X_C^\gamma$ ), using the system and experimental phase fractions below the  $M_S$  reported by Toji *et al.*<sup>[3]</sup> Black solid lines represent CCE, CCE $\theta$ , and BCE $\theta$  conditions (triangles, squares and circles, respectively). Blue dashed lines are recalculations of the initial carbon content of the system, as predicted by the reported  $X_{C,CCE\theta}^\gamma$  in Ref. [3] The red dashed line denotes the initial carbon content of the system. CCE $\theta$ \_Si, BCE $\theta$ \_Si, and  $X_{C-\mu_C}^0$  were calculated under PE allowing the partition of Si between  $\alpha'$  and  $\theta$ . Red crosses mark experimental measurements of carbon content in austenite (Color figure online).

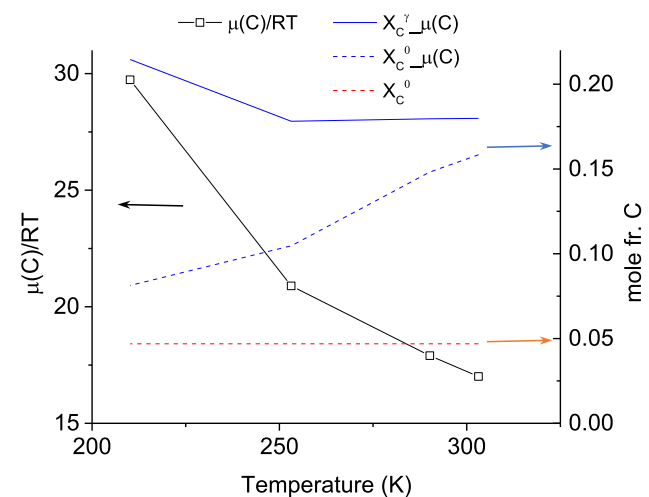


Fig. 2—Temperature variation of the paraequilibrium chemical potential of C ( $\mu_C$ ) in austenite in equilibrium with tempered martensite (solid black line, the ordinate at the left hand side). The carbon content of austenite ( $X_{C-\mu_C}^\gamma$ , blue solid line) and initial carbon content ( $X_{C-\mu_C}^0$ , blue dashed line) were recalculated from values of  $\mu_C$ . The red dashed line denotes the initial carbon content of the system (Color figure online).

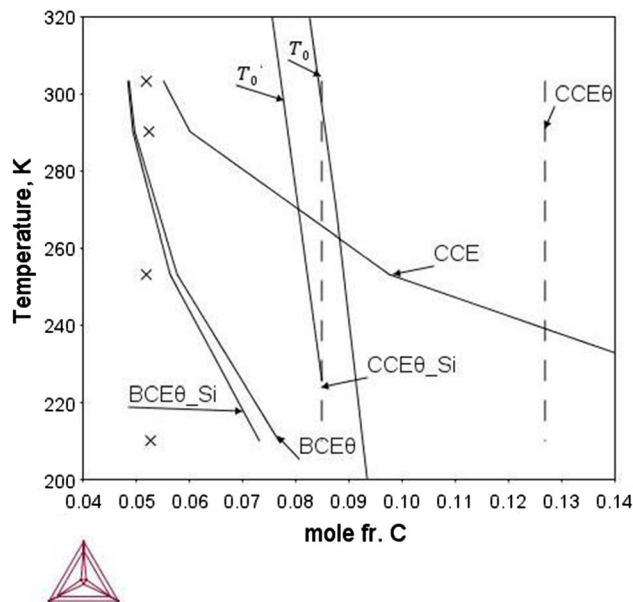


Fig. 3—Isoleth section of the phase diagram showing the calculations of  $X_C^\gamma$  according to both CCE and BCE $\theta$  models. Crosses denote experimental data by Toji *et al.*<sup>[3]</sup>

$X_C^\gamma - \mu_C$  in Figure 2), even higher than that predicted via CCE model at low temperatures (low  $f_V^\gamma$ ). It should be pointed out that according to the calculations under the imposed  $\mu_C^\alpha = \mu_C^\gamma$  condition,  $X_C^\gamma$  seems to slightly decrease with temperature, which ought to be related to the retrograde nature of  $X_C^{\gamma/\alpha}$  solvus line.<sup>[6]</sup>

Figure 3 shows the experimental data reported by Toji *et al.*<sup>[3]</sup> (crosses) compared with the predicted carbon content in austenite under CCE and BCE $\theta$  models, i.e., considering the mass balance. The data correspond to samples quenched at different temperatures and partitioned at the same temperature and time (673 K, 300 s). Figure 3 also includes the  $T_0$  and  $T_0'$  curves.  $T_0$  represents the compositions for equal Gibbs free energy of BCC and FCC phases, whereas  $T_0'$  is calculated with additional energy term to the BCC phase (400 Jmol<sup>-1</sup>). It is observed that the fit to the BCE $\theta$  predictions is reasonable at temperatures close to the  $M_S$ , whereas the experimental data do not correspond well to the BCE $\theta$  prediction at temperatures well below

the  $M_S$ . In the study by Toji *et al.*,<sup>[3]</sup> conversely, the experimental data fit better the CCE model for temperatures right below the  $M_S$ , but it is still far from their constant CCE $\theta$  prediction for lower temperatures. From the microstructural point of view, it is reasonable to expect a better fit of the experimental data to BCE $\theta$  (cf. Figure 3) because the phase distribution is much more accurately described in the BCE $\theta$  model than in the CCE model. However, the constant value of the experimental carbon content is still not understood. It has been suggested<sup>[7]</sup> that plate martensite has comparatively less defects than lath martensite; thus, carbon is forced to remain in the interstitial sites. The diffusion of C is consequently hindered and thus poor carbon redistribution, as the one experimentally reported by Toji *et al.*,<sup>[3]</sup> could be expected.

In summary, a modified model is proposed for the prediction of carbon content in austenite in Q&P treatment, which includes the mass balance of carbon into the  $\alpha' + \gamma + \theta$  equilibrium. According to the new model, it is pointed out that at temperatures below the  $M_S$  (i)  $X_C^\gamma$  should increase as the temperature decreases, and (ii)  $X_{C,CCE}^\gamma > X_{C,BCE\theta}^\gamma$ .

The authors are grateful for the support of ANID, Project No. 11170104 and to Prof G. Miyamoto, Tohoku University, for a valuable discussion.

## REFERENCES

1. J. Speer, D.K. Matlock, B.C. De Cooman, and J.G. Schroth: *Acta Mater.*, 2003, vol. 51, pp. 2611–22.
2. Y. Toji, H. Matsuda, M. Herbig, P.-P. Choi, and D. Raabe: *Acta Mater.*, 2014, vol. 65, pp. 215–28.
3. Y. Toji, G. Miyamoto, and D. Raabe: *Acta Mater.*, 2015, vol. 86, pp. 137–47.
4. Y. Toji, H. Matsuda, and D. Raabe: *Acta Mater.*, 2016, vol. 116, pp. 250–62.
5. D.P. Koistinen and R.E. Marburger: *Acta Metall.*, 1959, vol. 7, pp. 59–60.
6. G.J. Shiflet, J.R. Bradley, and H.I. Aaronson: *Metall. Trans. A*, 1978, vol. 9, pp. 999–1008.
7. G.R. Speich: *Trans. AIME*, 1969, vol. 245, pp. 2553–64.

**Publisher's Note** Springer Nature remains neutral with regard to jurisdictional claims in published maps and institutional affiliations.